Supplementary Online Material

Global mean metabolism uptake across patients' groups

The global mean scaling is generally accepted as the most appropriate scaling method for PET images in the Statistical Parametric Mapping (SPM) community (1-3). This scaling method assumes that detected putative local do not significantly affect the global mean glucose uptake. However, this assumption might be violated in patients with widespread hypometabolism patterns (3). Widespread areas of hypometabolism can lead to significant underestimation of the "healthy" global mean uptake and, therefore, to significant overestimation of the local uptake after proportional scaling (3). Thus, this effect can result in underestimating hypometabolic or overestimating hypermetabolic areas by voxel-based statistical evaluation. To investigate the presence of artifacts in our patients, we compared patients' and controls' global mean metabolism uptake, extracting the raw metabolic values from an FDG-PET-specific mask, as previously suggested (3). Therefore, we assumed hypermetabolism could be artifactual if the global mean value of metabolism uptake differed between the pre and post-COVID groups and the control group. We performed an ANOVA model with Bonferroni correction for multiple comparisons using the multcompare function in Matlab R2020b (MathWorks Inc.). The three groups showed comparable global metabolism uptake values (Table SX). Specifically, the comparison between all post-COVID (N=45), pre-COVID (N=15), and control (N=52) patients showed no significant differences (p=0.181).

Table S1. Global mean metabolism uptake across patients' groups

Group	Global Mean Metabolism	p-value* (patients vs. controls)	p-value* (pre vs. post-COVID)
Post-Covid (n=45)	20219.0 ± 7665.0	0.3959	0.3645
Pre-Covid (n=15)	23329.0 ± 7132.1	1.0000	
Controls (n=52)	22284.0 ± 5554.0	-	-

* ANOVA with Bonferroni post hoc multiple comparison tests

Table S2. Main ^{18}F-FDG PET hypometabolism in post-COVID scans compared to control scans (p-voxel < 0.05, p-cluster < 0.05 FWE corrected).

Cluster		Voxel	MNI coordinates			Localization
K	$P_{FWE\text{-}corr}$	T-score	X	y	z	
31627	< 0.001	3.90	-14	-84	-15	Left Occipital Fusiform Gyrus
		3.90	-12	-74	-9	Left Lingual Gyrus
		3.73	-6	-72	25	Left Precuneus Cortex
		3.65	8	-62	23	Right Precuneus Cortex
		3.53	42	-86	35	Right Lateral Occipital Cortex
		3.49	-36	-86	33	Left Lateral Occipital Cortex
		3.28	46	-36	69	Right Parietal Lobe
		3.28	-40	-74	37	Left Parietal Lobe
		3.27	12	-96	-15	Right Occipital Lobe
		3.13	-30	-100	7	Left Occipital Lobe
		3.09	52	-64	41	Right Parietal Lobe
		3.04	46	28	43	Right Frontal Lobe
		3.00	-10	-66	11	Left Occipital Lobe
		2.92	-2	-64	37	Left Parietal Lobe
		2.90	-26	-74	51	Left Parietal Lobe
		2.82	-60	-56	31	Left Parietal Lobe

The k-value represents the number of voxels inside a particular cluster. MNI, Montreal Neurological Institute. MNI coordinates are expressed in mm. Table shows 16 local maxima more than 4 mm apart.

Table S3. Main [18]F-FDG PET hypo- and hypermetabolism in post-COVID scans compared to pre-COVID scans (paired samples t-test, p-voxel < 0.05, p-cluster < 0.05 FWE corrected) between 2 and 6 months after COVID-19 infection onset (n=6).

Cluster		Voxel	MNI coordinates			Localization
k	$P_{FWE\text{-}corr}$	T-score	X	y	z	
Hypometabolism						
44313	< 0.001	10.76	46	-2	37	Right Precentral Gyrus
		10.21	46	-90	-17	Right Occipital Lobe
		8.77	20	-42	-11	Right Lingual Gyrus
		8.10	70	-52	-5	Right Middle Temporal Gyrus
		7.87	36	-68	27	Right Lateral Occipital Cortex
		6.94	12	6	73	Right Superior Frontal Gyrus
		6.77	42	-94	11	Right Occipital Pole
		6.70	-14	-68	45	Left Precuneus Cortex
		6.66	-26	-66	63	Left Lateral Occipital Cortex
		6.42	-48	-44	31	Left Supramarginal Gyrus
Hypermetabolism						
7990	0.016	10.31	-34	46	-21	Left Frontal Pole
		10.17	-32	50	-19	Left Frontal Pole
		8.00	-20	6	-25	Left Temporal Pole
		7.60	-12	-38	-17	Left Cerebellum
		7.51	-34	36	-25	Left Frontal Pole
		7.03	-36	6	-11	Left Insular Cortex
		6.82	-32	-16	-13	Left Temporal Lobe
		6.69	26	-2	-17	Right Amygdala
		6.57	-26	-12	-15	Left Hippocampus
		6.23	-8	-40	-15	Left Cerebellum

The k-value represents the number of voxels inside a particular cluster. MNI, Montreal Neurological Institute. MNI coordinates are expressed in mm. Table shows 10 local maxima more than 4 mm apart for each contrast.

Table S4. Significant positive correlations between age and regional ^{18}F-FDG PET hypo- and hypermetabolism in post-COVID patients in comparison with controls (p-voxel < 0.05, p-cluster < 0.05 FWE corrected).

Cluster		Voxel	MNI coordinates			Localization
k	$P_{\text{FWE-corr}}$	T-score	x	y	z	
Hypometabolism						
46148	< 0.001	6.39	6	36	9	Frontal Lobe
		6.24	12	16	3	Caudate Head
		6.07	-2	10	39	Frontal Lobe
		6.00	6	22	25	Frontal Lobe
		5.84	4	14	41	Frontal Lobe
		5.76	-42	14	-13	Frontal Lobe
		5.57	0	-10	35	Cingulate Gyrus
		5.51	-26	-6	69	Superior Frontal Gyrus
		5.51	-8	16	-1	Caudate Head
		5.42	-12	6	11	Caudate Head
		5.41	-10	10	7	Caudate Head
		5.34	16	2	13	Internal Capsule
		4.71	48	14	-7	Insula
		4.51	50	-38	3	Middle Temporal Gyrus
		4.50	4	-20	5	Thalamus
		4.41	64	12	27	Frontal Lobe
Hypermetabolism						
27581	< 0.001	6.66	-28	-62	-41	Cerebellar Hemisphere
		6.66	-18	-24	51	Temporal Lobe
		6.06	26	-64	-39	Cerebellar Hemisphere
		5.26	-36	-12	21	Frontal Lobe, Primary Motor
		4.42	-42	-24	25	Frontal Lobe
		4.31	6	-56	-25	Vermis
		4.30	-14	-64	41	Parietal Lobe, Precuneus

	4.13	20	-14	-5	Corticospinal Tract
	4.08	-34	-78	-59	Cerebellar Hemisphere
	3.93	-20	-108	-1	Occipital Lobe
	3.91	-16	-14	-1	Corticospinal Tract
	3.83	-14	-52	47	Parietal Lobe, Precuneus
	3.51	50	-70	-39	Cerebellar Hemisphere
	3.42	-48	-88	1	Occipital Lobe
	3.38	-68	-10	27	Frontal Lobe
	3.18	-24	-106	-9	Occipital Lobe

Table S5. Significant positive correlations between the presence of neurological symptoms at the time of imaging and regional ^{18}F-FDG PET hypo- and hypermetabolism in post-COVID patients in comparison with controls (p-voxel < 0.05, p-cluster < 0.05 FWE corrected).

Cluster		Voxel	MNI coordinates			Localization
k	$P_{FWE\text{-}corr}$	T-score	x	y	z	
Hypometabolism						
14020	< 0.001	3.64	-34	-90	31	Occipital Lobe
		3.62	-32	-90	35	Occipital Lobe
		3.59	62	-66	15	Occipital Lobe
		3.44	70	-28	19	Frontal Operculum
		3.42	-36	-88	35	Occipital Lobe
		3.35	-38	-88	31	Occipital Lobe
		3.13	-42	-74	25	Occipital Lobe
		3.07	50	-56	37	Parietal Lobe
		2.86	50	-24	35	Parietal Lobe
		2.85	54	-22	37	Parietal Lobe
		2.82	58	-22	41	Parietal Lobe
		2.76	58	-44	31	Parietal Lobe
		2.72	44	-70	25	Parietal Lobe
		2.66	-40	-58	61	Parietal Lobe
Hypermetabolism						
19067	< 0.001	5.18	-24	-28	-23	Temporal Lobe
		4.52	6	-18	-41	Pons
		4.39	2	-16	-39	Pons
		4.26	-12	2	-19	Temporal Lobe
		4.17	-2	-16	-37	Pons
		4.16	4	-38	-57	Medulla
		4.15	22	-4	-37	Temporal Lobe
		4.12	10	-34	-47	Medulla

	4.08	-22	-6	-39	Temporal Lobe
	3.94	-4	-16	-21	Corticospinal Tract
	3.85	-50	-70	-31	Cerebellum
	3.64	8	12	-27	Frontal Lobe
	3.55	6	-34	-25	Cerebellum
	3.47	-48	-74	-29	Cerebellum
	3.47	50	-24	-9	Temporal Lobe
	3.45	-44	28	-21	Frontal Lobe

Table S6. Significant positive correlations between SARS-CoV-2 infection severity scores and regional ^{18}F-FDG PET hypo- and hypermetabolism in post-COVID scans compared to pre-COVID scans (p-voxel < 0.05, p-cluster < 0.05 FWE corrected).

Cluster		Voxel	MNI coordinates			Localization
k	$P_{FWE\text{-}corr}$	T-score	x	y	z	
Hypometabolism						
34105	< 0.001	5.01	24	-14	57	Precentral Gyrus
		4.87	8	24	59	Superior Frontal Gyrus
		4.87	-22	12	53	Superior Frontal Gyrus
		4.44	2	10	31	Cingulate Gyrus, anterior division
		4.43	-6	14	67	Superior Frontal Gyrus
		4.19	-8	12	71	Superior Frontal Gyrus
		4.10	-12	-18	77	Precentral Gyrus
		4.09	12	-6	73	Superior Frontal Gyrus
		3.89	34	-22	69	Precentral Gyrus
		3.88	-12	-2	77	Superior Frontal Gyrus
		3.82	-10	-8	75	Superior Frontal Gyrus
		3.77	66	0	15	Precentral Gyrus
		3.75	-24	-28	73	Postcentral Gyrus
		3.75	-32	-54	33	Superior Parietal Lobule
		3.64	30	2	57	Middle Frontal Gyrus
		3.55	24	-54	-1	Lingual Gyrus
Hypermetabolism						
22254	< 0.001	5.49	22	26	-13	Frontal Orbital Cortex
		4.86	-24	4	-17	Frontal Orbital Cortex
		4.77	2	-52	5	Precuneus Cortex
		4.60	-38	-48	-27	Temporal Occipital Fusiform Cortex
		4.48	-16	-40	-37	Frontal Lobe

	4.28	14	8	27	WM Callosal body
	4.26	-20	-56	15	Precuneus Cortex
	4.24	-16	8	37	WM Callosal body
	4.15	-4	26	15	Cingulate Gyrus, anterior division
	4.07	-52	-44	-35	Frontal Lobe
	4.02	28	40	-3	Frontal Pole
	3.98	48	24	-27	Temporal Pole
	3.93	-32	-32	27	WM Superior longitudinal fascicle
	3.93	16	-44	-33	Cerebellum
	3.91	42	-28	-5	Middle Temporal Gyrus, posterior division
	3.82	30	30	-3	Frontal Orbital Cortex

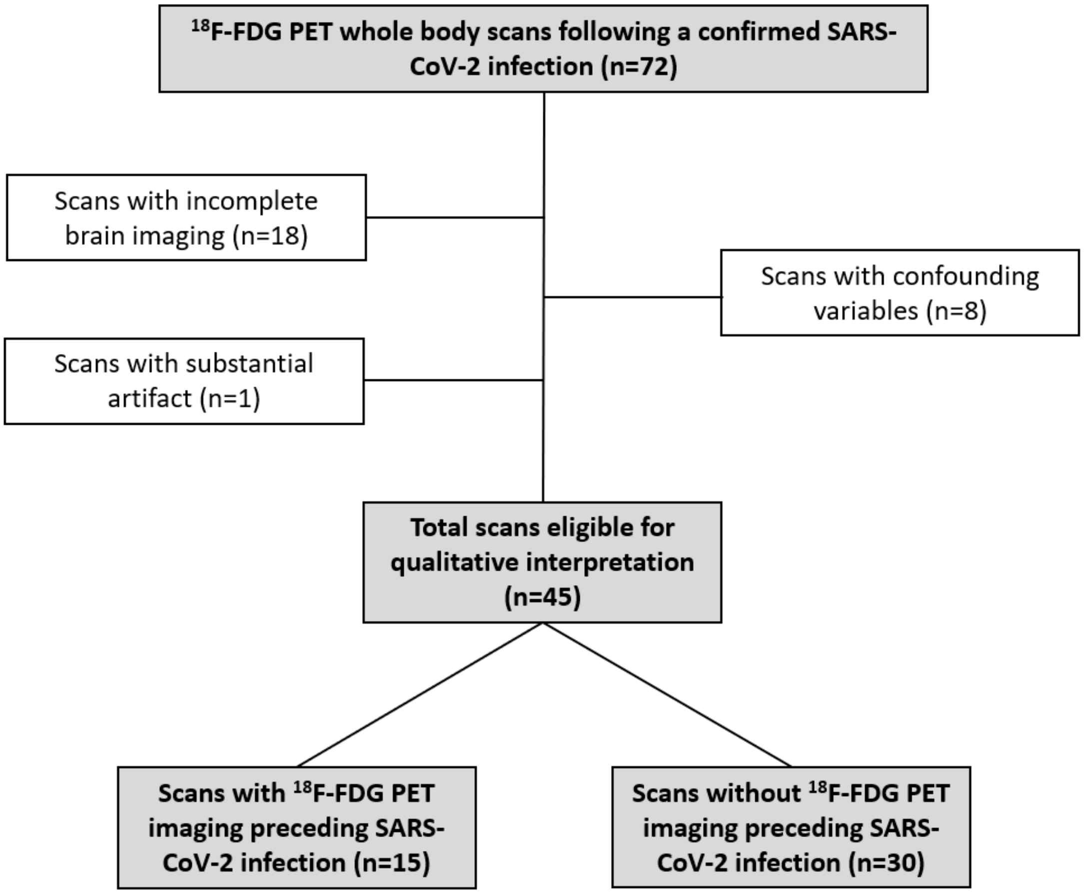

Fig. S1- Study flow diagram.

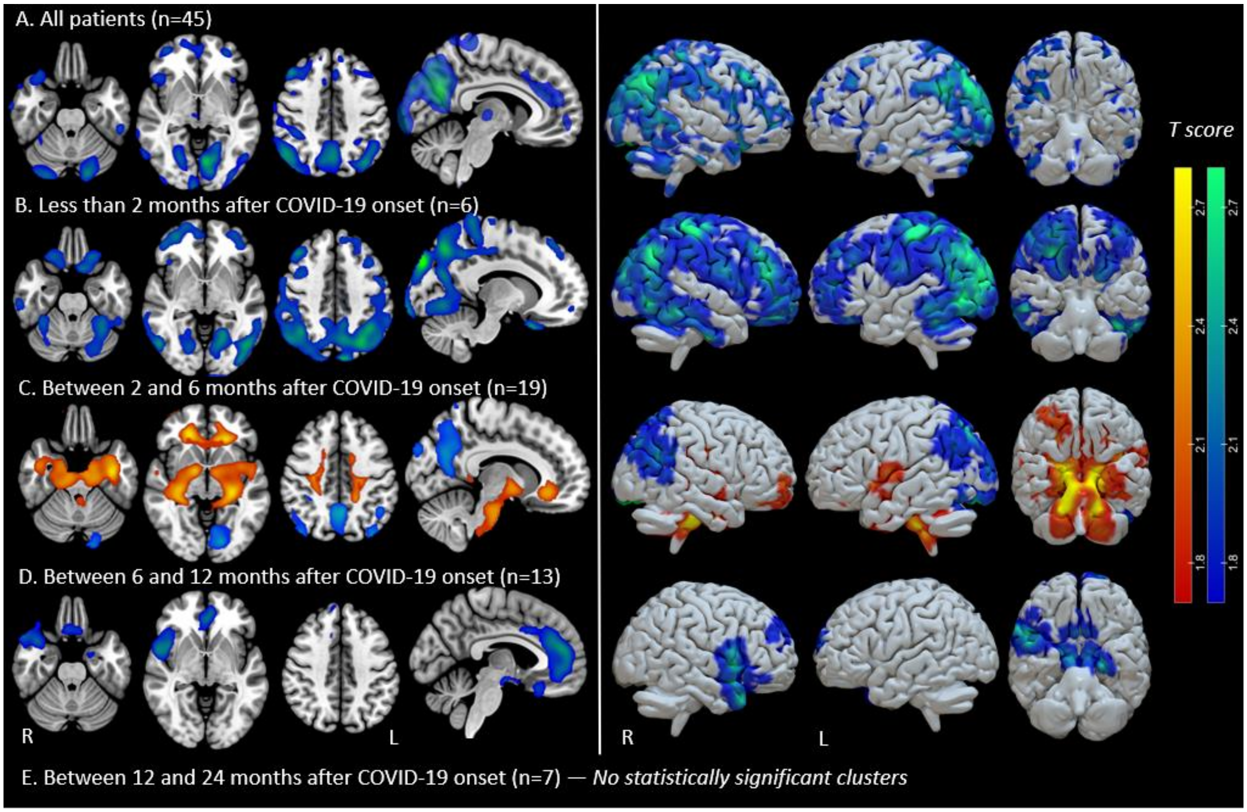

Fig. S2- SPM analysis of 18F-FDG PET metabolic group differences. Hot and cool color scales show regions with hypermetabolism and hypometabolism, respectively. The SPM t-maps are projected onto a surface rendering and axial views of the customized MRI template (p-voxel < 0.05 uncorrected, p-cluster < 0.05 FWE- corrected). A, Whole group of post-COVID (n=45) vs. control scans (n=52) analysis demonstrates significant hypometabolism in the bilateral frontal, parietal, occipital, posterior temporal lobes and cerebellum. B-E, Post-COVID patients were further sub-grouped according to the time delay between the positive RT-PCR and PET imaging: 0-2 (B), 2-6 (C), 6-12 (D), and greater than 12 months (E). Two months after COVID-19 onset, extensive neocortical hypometabolism predominantly involving the bilateral parietal, posterior temporal, and frontal lobes was noted on post-COVID scans (B, n=6). Decreased extent of hypometabolism was observed between 2 and 6 months, with persistent involvement of the bilateral parietal lobes (C, n=19). Between 6 and 12 months after the infection, hypometabolism was limited to the mediofrontal, including the anterior cingulate gyrus, posterior rectus gyrus, and right anterior temporal lobe (D, n=13). After 12 months, no clusters survived correction for multiple comparisons (n=7). Significant hypermetabolism with central cerebral involvement was only observed 2-6 months after the infection (C).

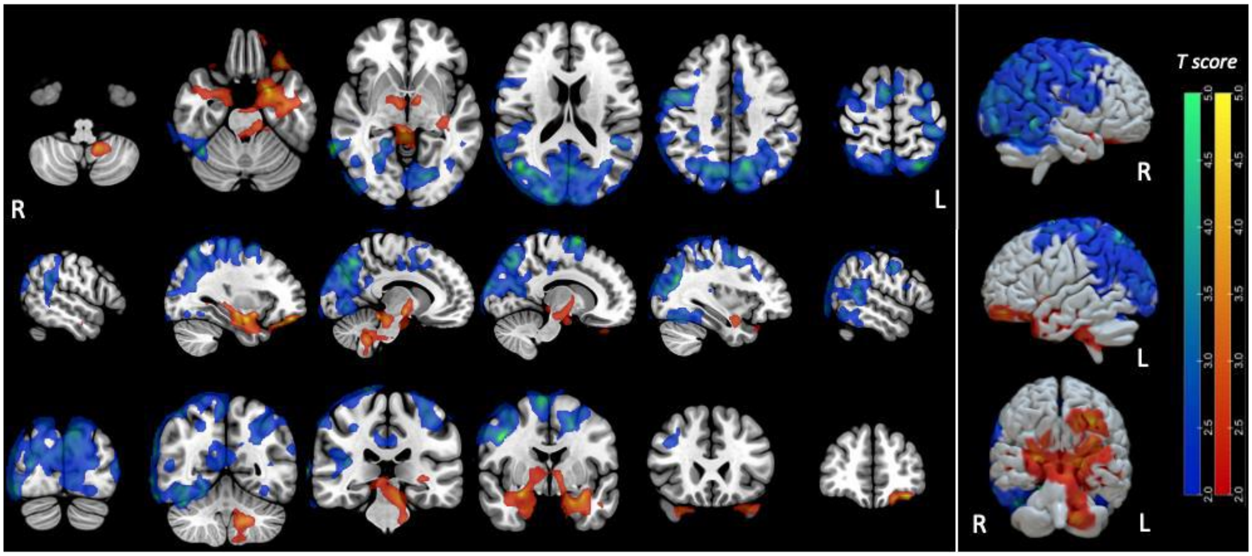

Fig. S3- Regional 18F-FDG PET hypo- and hypermetabolism in post-COVID scans compared to pre-COVID scans (paired samples t-test, p-voxel < 0.05, p-cluster < 0.05 FWE corrected) between 2 and 6 months after COVID-19 infection onset (n=6). Hot and cool color scales show regions with hypermetabolism and hypometabolism, respectively.

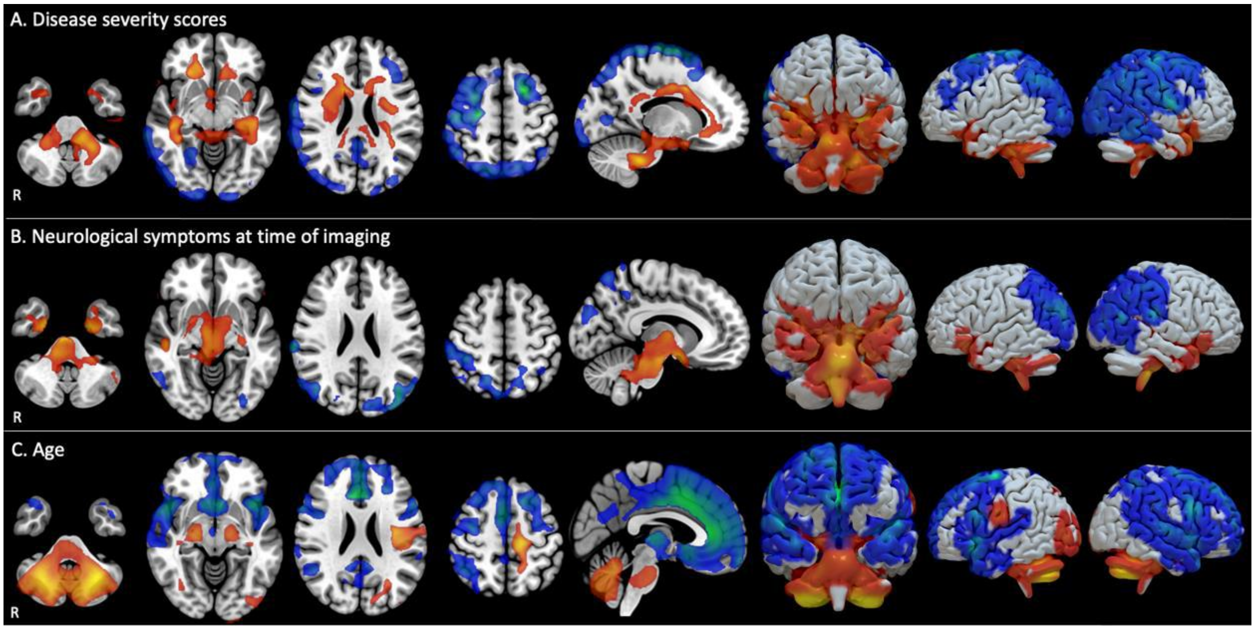

Fig. S4- Significant positive correlation of SARS-CoV-2 disease severity scores, neurological symptoms at the time of imaging, and age with regional [18F]-FDG PET hypo- and hypermetabolism in post-COVID scans compared to control scans. SPM T maps are displayed with a hot color scale for brain hypermetabolism and with a cool color scale for brain hypometabolism (p-voxel < 0.05, p-cluster < 0.05 FWE corrected).

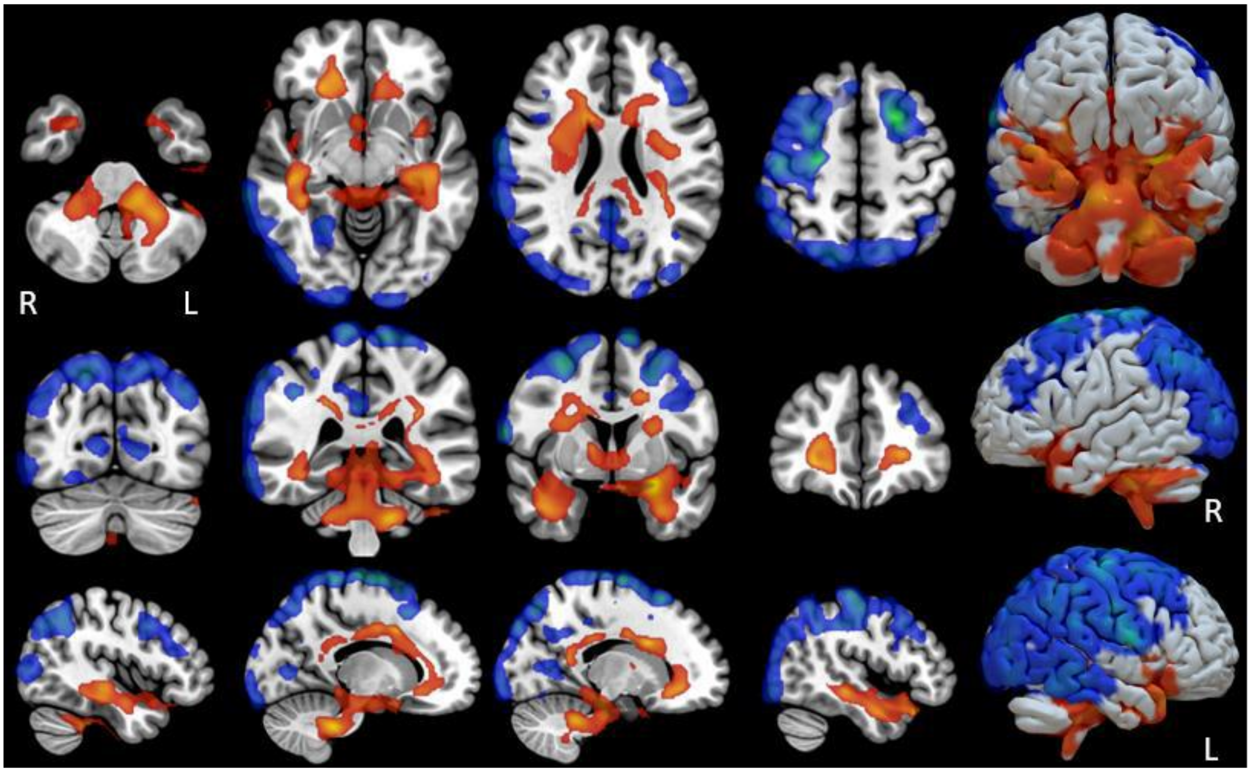

Fig. S5- Significant positive correlations between SARS-CoV-2 infection severity scores and regional 18F-FDG PET hypo- and hypermetabolism in post-COVID scans compared to pre-COVID scans. SPM T maps display a hot color scale for brain hypermetabolism and a cool color scale for brain hypometabolism (p-voxel < 0.05, p-cluster < 0.05 FWE corrected).

References

1. Friston KJ. Statistical Parametric Mapping. In: Kötter R, ed. Neuroscience Databases: A Practical Guide. Boston, MA: Springer US, 2003; p. 237-250.

2. Buchert R, Wilke F, Chakrabarti B, Martin B, Brenner W, Mester J, Clausen M. Adjusted scaling of FDG positron emission tomography images for statistical evaluation in patients with suspected Alzheimer's disease. J Neuroimaging 2005;15(4):348-355. doi: 10.1177/1051228405280169

3. Martini AL, Carli G, Kiferle L, Piersanti P, Palumbo P, Morbelli S, Calcagni ML, Perani D, Sestini S. Time-dependent recovery of brain hypometabolism in neuro-COVID-19 patients. Eur J Nucl Med Mol Imaging 2022;50(1):90-102. doi: 10.1007/s00259-022-05942-2